2019-11

Epibenthic community variation along an acidified tropical estuarine system

Hossain, MB

6

Biomonitoring acidification using marine gastropods

8

9 David J. Marshall[1]*, Ahmed Awad Abdelhady[2], Dennis Ting Teck Wah[1], Nurshahida

10 Mustapha[1], Stefan H. Gödeke[3], Liyanage Chandratilak De Silva[4], Jason M. Hall-Spencer[5,6]

11

12 [1]Environmental and Life Sciences, Faculty of Science, Universiti Brunei Darussalam, Brunei

13 Darussalam; [2]Geology Department, Faculty of Science, Minia University, El-Minia 61519,

14 Egypt; [3]Geological Sciences, Faculty of Science, Universiti Brunei Darussalam; [4]Faculty of

15 Integrated Technologies, Universiti Brunei Darussalam; [5]School of Biological and Marine

16 Sciences, University of Plymouth, UK; [6] Shimoda Marine Research Center, Tsukuba

17 University, Japan.

18

19 *Corresponding author: David J. Marshall, Environmental and Life Sciences, Faculty of

20 Science, Universiti Brunei Darussalam, Jalan Tungku Link, BE1410, Gadong, Brunei

21 Darussalam. Email: david.marshall@ubd.edu.bn; Tel.: +673 8974143

22

23

24

25

26

27

28

29

30

31

32

Abstract

Ocean acidification is mainly being monitored using data loggers which currently offer limited coverage of marine ecosystems. Here, we trial the use of gastropod shells to monitor acidification on rocky shores. Animals living in areas with highly variable pH (8.6 - 5.9) were compared with those from sites with more stable pH (8.6 - 7.9). Differences in site pH were reflected in size, shape and erosion patterns in *Nerita chamaeleon* and *Planaxis sulcatus*. Shells from acidified sites were shorter, more globular and more eroded, with both of these species proving to be similarly good biomonitors. After an assessment of baseline weathering, shell erosion can be used to indicate the level of exposure of organisms to corrosive water, providing a tool for biomonitoring acidification in heterogeneous intertidal systems. A shell erosion ranking system was found to unequivocally discriminate between acidified and reference sites. Being spatially-extensive, this approach can identify coastal areas of greater or lesser acidification. Cost-effective and simple shell erosion ranking is amenable to citizen science projects and could serve as an early-warning-signal for natural or anthropogenic acidification of coastal waters.

Keywords: ocean acidification; bioindicators; acid sulphate soils; calcification; snails; tropical

1. Introduction

Monitoring changes in the corrosiveness of seawater is crucial to managing and predicting the impact of ocean acidification. The past two decades have seen an increase in the global deployment of fixed buoys equipped with instruments and data-loggers. These monitoring stations capture long-term changes in seawater chemistry but are costly to implement and maintain, and provide data from discrete points. Biomonitoring may provide a complementary method for assessing acidification in coastal waters. Shelled gastropods can be useful biomonitoring organisms (Gibbs et al., 1987; Phillips and Rainbow, 1993; Zhou et al., 2008; Nuñez et al., 2012, Márquez et al., 2015; Proum et al., 2016; Begliomini et al., 2017) and so oceanographers have begun to use pteropod shell dissolution to assess the effects of acidification in the open sea (Bednaršek et al., 2012a, 2012b, 2014). Here, we propose an

approach using benthic gastropods to assess acidification impacts in shallow-water coastal habitats.

Studies of benthic gastropods have contributed significantly to our understanding of the ecological consequences of ocean acidification (Lardies et al., 2014; Garilli et al., 2015). Much of this work has focussed on the energetic costs of calcification in acidified water (Chen et al., 2015; Harvey et al., 2016, 2018; Connell et al., 2017; Duquette et al., 2017; Doubleday et al., 2017; Harvey et al., 2018). Gastropod shell mineralogy, dissolution and gross shell deformities are well documented, especially for CO_2 seep systems (Hall-Spencer et al., 2008; Chen et al., 2015; Duquette et al., 2017), yet no studies have assessed how well these features record episodes when seawater becomes corrosive to shells and skeletons.

Fluctuations in carbonate chemistry in near-shore marine environments arise from multiple natural and anthropogenic processes, with a major influence from the land via rivers, estuaries and sediments (Zhai et al., 2015). Carbonate undersaturation in coastal waters can be caused by flooding and reduced salinities, or eutrophication (Cai et al., 2011 a, b; Duarte et al., 2013; Zhai et al., 2015). Coastal acidification also develops through geochemical discharge from acidic soils (Powell and Martens, 2005; Grealish and Fitzpatrick, 2013). In Brunei (Borneo, South East Asia), a combination of eutrophication, peat swamp leachate, acidic pollutants and acid sulphate soils cause coastal acidification (Marshall et al., 2008; Grealish and Fitzpatrick, 2013; Proum et al., 2016, 2018), reducing biodiversity and affecting ecosystem functions (Marshall et al., 2016, 2018). A steep pH gradient in the Brunei estuarine system has been used to assess marine organism and community responses to acidification (Bolhuis et al., 2014; Hossain and Marshall, 2014; Majewska et al., 2017; Proum et al., 2017).

Gastropod snails with heavily corroded shells inhabit the rocky intertidal zone on the open coast of Brunei, away from influence of the estuarine system. Here we investigated the effect of acidic water discharge on rocky shore seawater pH. We then tested whether gastropods can be used to inform about corrosive water conditions on rocky shores, by comparing between responses to acidified and normal seawater exposure using two species. An overarching objective was to appraise methods using shells of benthic gastropods to monitor corrosive seawater events.

2. Materials and Methods

2.1 Geology and study sites

The South China Sea coast of Brunei Darussalam has sandstone ridges separated by clay sediments containing pyrite (FeS_2) and pyritic minerals (Morley et al., 2003) which react when exposed to oxygen according to the equation:

$$2\ FeS_2 + 7\ O_2 + 2\ H_2O => 2\ Fe^{2+} + 4\ SO_4^{2-} + 4\ H^+$$
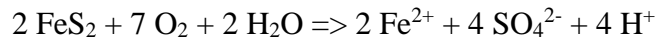
This lowers the pH of water that flows from the land into the South China Sea (Grealish and Fitzpatrick, 2013) (Fig. 1). Water enters the coastal ecosystem via tributaries and watercourses, or through discharges of submarine or subterranean groundwater, which can be below pH 4 (Azhar et al., 2019; Waska et al., 2019; Fig. 1). Topography, tides, currents and waves influence the area of seawater affected by groundwater discharge (Urish and McKenna, 2004; Waska et al., 2019).

Eight sites were selected based on the occurrence of *Nerita chamaeleon* Linnaeus, 1758 (Neritoidea) and *Planaxis sulcatus* (Born, 1778) (Cerithioidea) and on the presence of intertidal acidic water discharge (Fig. 1). Three sites were strongly influenced by acidified water (E1, E2 and E3; A1) whereas the reference sites were not (JPMC, PJER, PUN, TP, UB). PUN and E1-3 were natural rocky shores, whereas the others were artificial seawalls (Fig. 1, A1). At low tide E1-3 had acidified water running over mixed sand and boulders exposing both species of gastropod to acidified water although when the tide was in, seawater pH and salinity were normal (Grealish and Fitzpatrick, 2013; A1). Sites were separated by km scale distances, except E1-3 which were approximately > 100 m apart. Physicochemical characteristics, such as temperature and oxygen content, were similar across the sites.

2.2 Sampling

A total of 124 water samples (40 ml, between 9-32 per site) were collected from snail habitat in the intertidal zone on thirteen trips in April-July 2018. Samples were taken to measure pH and salinity ranges during low-tide, including from small pools on the high shore, and from the open sea on the low shore. Sometimes small water-bodies were sampled with a syringe. On return to the laboratory, water parameters were measured at 24°C, the laboratory and night-time field temperature. Salinity was measured using a Hach multi-meter (model HQ40d) with an Intellical probe (Hach Lange GmbH Headquarter, Düsseldorf, Germany). pH was measured using a Mettler Toledo pH transmitter 2100e and probe (Mettler-Toledo GmbH, Giessen, Germany) calibrated with pH 4.00 and 7.00 CertiPUR Merk buffers traceable to SRM from

NIST. Repeated measures of the same sample yielded a reading precision of $\pm\ 0.012\ (\text{s. d.}, \text{n} = 10)$.

Nerita chamaeleon and *P. sulcatus* are common on rocky-shores in this region of Asia. Individuals of both species occupy hard-substrata, intertidal pools, and sometimes soft sediments between boulders, across a broad mid-tidal zone (approximately 0.5-1.5 m Chart Datum). Abundance in both cases can exceed 50 snails per m^2. The species differ greatly in shell shape with the shell of *N. chamaeleon* expanded diametrical and compressed axially and that of *P. sulcatus* expanded axially (Figs. 2 and 3). Similar-sized living adults (20-30 mm for both species) were collected and analysed between Dec 2016 and Jul 2018. Snails of *N. chamaeleon* (n = 132) and *P. sulcatus* (n = 147) were stored in 70% ethanol within an hour of collection. Shell size, shape and surface erosion were then measured or ranked.

We compared between the reference and acidified sites using attributes of either species. The same attribute was not always determined for both species, with shell shape often dictating the approach followed. For example, it was not feasible to assess shell shape variation using conventional geometric morphometric landmarks in the case of the globular-shaped *Nerita chamaeleon*, which has severely compressed spire whorls.

2.3 Size, mass and shell shape

Shell height, aperture length, dry shell mass and dry soft tissue mass were measured for *N. chamaeleon* from E1 (acidified) and PUN (reference) (Fig. 1). After photographing apertural and abapertual shell surfaces (Canon EOS 5D, Mark II, 100 mm macrolens), length was measured using Olympus CellSens software (A2). Shells were then cracked open and separated from soft tissues. Following oven-drying at 70°C for three days, the tissue was weighed with a balance accurate to 0.001 g.

Shell length and mass data were scaled to a common aperture length (Marshall et al., 2008, A2). As shell morphology varies allometrically, measurements were converted to natural logarithms before fitting ordinary least squares regressions to plots (Sigmaplot ver. 14, Systat Software, Inc., New York, US). The effect of site (PUN and E1) was assessed using Generalized Linear Models for normal distribution with a log-link function (Statistica ver. 12, StatSoft, New York, US).

Shell shape analyses of *P. sulcatus* used samples from E2 (acidified), TP and UB (reference), and followed methods described by Abdelhady et al. (2018). Each individual was photographed

154 (> 20 per site) and twenty landmarks of the shell were digitized using the TPSDig Package

155 (http://life.bio.sunysb.edu/morph/, Rohlf, 1996; A3). The error associated with capturing 2D

156 image from 3D object was minimized (see Abdelhady, 2016). Generalized Procrustes Analysis

157 was applied to these data using the method of Rohlf and Slice (1990) to ensure that distances

158 among homologous landmarks were minimized such that the resulting data best represented

159 the shape. Procrustes residual data were projected to Detrended Corresponding Analysis

160 (DCA) to arrange the shell shape data on coordinates (see Abdelhady and Fürsich, 2014, 2015).

161 Analysis of Similarities (ANOSIM) was applied to test the null hypothesis that similarities

162 between sites are smaller or equal to similarities within sites. Finally, Thin Plate Spline was

163 used to assess changes in shell shape between specimens (see Zelditch et al., 2012). Statistical

164 analyses were carried out using PAST version 2.17c (Hammer et al., 2001, 2006).

165 *2.4 Shell surface erosion*

166 Shell erosion areas, representing lifetime exposures, were assessed quantitatively or using a

167 ranking system. Two methods were used to quantify erosion areas from photographs of the

168 abapertural side of *N. chamaeleon* collected from PUN (reference) and E1 (acidified) in Dec

169 2016. Our first method involved manually demarcating and calculating planar surface area (2D)

170 of erosion down to the light grey, fine-textured layer using an Olympus CellSens drawing tool

171 (A2). The eroded area was then expressed as a proportion of the total surface area of the shell.

172 Generalized Linear Models for a normal distribution and log-link function (Statistica ver. 12,

173 StatSoft, New York, US) were used to assess the effect of acidification. For each site, we

174 counted the number of individuals showing no erosion as well as those showing eroded surfaces

175 of > 10% of the total area.

176 Inaccuracies in delineation of areas arose when erosion occurred in the fine grooves of shells

177 (A2), so we applied a second method to *N. chamaeleon* shells based on digital pixel analysis.

178 We developed software that used k-mean clustering, which assigns observations to clusters

179 using Mahalanobis distance measures. We grouped our data into background (white colour),

180 eroded shell surfaces (light colour) and unaffected shell surfaces (dark colour). The digital

181 method was then compared with our manual assessment of eroded areas using a linear

182 regression (Statistica ver. 12).

183 Shell Erosion Ranks (SERs) were determined for both species (Figs 2 and 3) using different

184 criteria for pragmatic reasons (shell shape). For *N. chamaeleon*, erosion ranks were based on

185 apical images of the shell. The image was divided into seven sectors, each representing a

186   different shell age (Fig. 2). A 0 – 7 rank, based on the highest numbered sector with > 50%

187   surface erosion was determined for two types of erosion. Type I was deep erosion to

188   homogenous non-pigmented fine-textured shell and Type II was superficial erosion of the outer

189   'prismatic' layer containing slight ridges and pigmented shell. Our analyses were based on

190   either the rank for Type I (0-7) or that for both types summed to give a final rank between 0 –

191   14 (Fig. 2). A shell that was completely covered by periostracum was scored zero. In *P.*

192   *sulcatus*, shell erosion was ranked using abapertural and apertural photographs (see Fig. 3 for

193   details of the abapertural ranking method). Data were statistically analysed using Generalized

194   Linear Models with a probit function for an ordinal multinomial distribution (Statistica ver.

195   12). Median scores and frequency distributions of ranks were plotted.

3. Results

3.1 Habitat pH and salinity

198   Upper pH values were similar for all stations (mean max pH ± s.d. = 8.50 ± 0.08, n = 6). pH

199   ranges were 8.56 - 7.90 (n = 63) for the reference sites and 8.60 - 5.93 (n = 61) for the acidified

200   sites (Fig. 4). Salinities were 33.2–20.2 for the reference sites and 32.8 - 0.2 for the acidified

201   sites. In a nearby estuary, lower pH and salinity generated through acidic groundwater

202   discharge causes calcite (Ca) and aragonite (Ar) undersaturation, and so snails at our acidified

203   sites (E1-3) are likely to experience corrosive water exposure (Fig. 4, bottom panel).

3.2 *Size, mass and shape*

205   Shells of *N. chamaeleon* from the acidified site were shorter than those at the reference site

206   (A4; Wald stat = 12.88, p= 0.0003). Shell and dry tissue mass did not differ significantly

207   between the sites (Wald stat = 3.42, p = 0.064 and Wald stat = 0.15, p = 0.694, respectively;

208   A4). In the shape analysis of *P. sulcatus*, cumulative plots of the average sizes confirmed the

209   suitability of using ~20 specimens with little change in this average when more specimens were

210   added. Reference-site *P. sulcatus* had similar shell shapes whereas the acidified-site specimens

211   had a larger width/height ratio (ANOSIM; p < 0.01; Fig. 5). DCA confirmed that acidified-site

212   snails had shorter shells with larger apertures. Shell shapes were similar for the reference

213   populations, which differed from the acidified population (DC1 versus DC2, Fig. 5). Apertures

214   were rounder (DC1 versus aperture shape; r = 0.44; Fig. 5) and shells were more globular in

215   acidified conditions (DC2 versus shell height; r = - 0.48; Fig. 5).

3.3 Shell surface erosion

217   Shells from acidified sites were more eroded than those at reference sites (Fig. 6). Differences

218   were found for manually-calculated absolute areas and areas relative to the total shell surface

219   (Fig. 6 A, B, C; $p < 0.001$). The average amount of eroded surface of acidified site snails was

220   $> 40\%$, compared to $< 10\%$ in reference site snails (Fig. 6). Only one acidified site snail had

221   no dissolution (Fig. 6 D).

222   In our digital technique, surface erosion areas were coloured red *vs* blue for unaffected areas

223   (Fig. 7). Results from our automated approach and our manual calculations were closely

224   correlated ($r = 0.91$; $p < 0.05$; Fig. 7), though the manual method underestimated eroded areas

225   in shell grooves. Due to its simplicity, the automated technique could be used for large sample

226   analysis although visual checks are needed, such as when the colour of eroded shell areas is

227   similar to that of uneroded areas.

228   Shell Erosion Ranks (SERs) indicated much more extensive erosion at the acidified sites (Figs

229   8 and 9). Reference site *N. chamaeleon* had a median SER of 5 whereas snails from acidified

230   sites had a rank of 10. There were however differences within the groups of reference or

231   acidified sites; PUN shells had greater erosion than JPMC and PJER, and E1 and E2 had more

232   erosion than E3 (Fig. 8 A; Table 1). SER frequencies were highly discriminatory in that ranks

233   of 5 and 6 (Type I), representing the most severe erosion, were only found at the acidified sites

234   (Fig. 8 B). These patterns were repeated in *P. sulcatus* with a median erosion rank of ~ 6.5 at

235   the reference sites compared with ~ 9 for the acidified sites (Fig. 9; Table 1). Whereas most of

236   the snails at the acidified sites had erosion ranks > 5, the highest rank recorded at the reference

237   sites was 4 and none of the snails at the acidified sites ranked 2 or less (Fig. 9 B). High

238   frequencies of the unique highest (or higher) erosion ranks were found at the acidified sites;

239   ranks 5 or 6 for *N. chamaeleon* collectively contributed more than 0.4 of all individuals and

240   rank 5 for *P. sulcatus* contributed around 0.6 of these populations.

4. Discussion

242   Gastropod shells have been used to monitor spatial patterns of acidification in oceanic pelagic

243   systems (Bednaršek et al., 2012a, 2012b, 2014) but not in coastal ecosystems. We found that

244   acidification of a rocky intertidal system was reflected in the shell attributes of two gastropod

245   species, with shell surface erosion patterns correlating with acidification.

246   Groundwater discharge affected open coast rocky shores of the region, with some rockpools as

247   low as pH 5.9, adding to previous observations of the effects of acidification on the ecology of

248   an estuarine system in Brunei (Marshall et al. 2008, 2016; Bolhuis et al., 2014; Hossain et al.,

249 2014; Majewska et al., 2017; Proum et al., 2017, 2018). Land-to-sea acidification via

250 submarine groundwater flux or water-course infiltration had little effect on pH at the reference

251 sites compared to that of direct discharge at the acidified sites (Urish and McKenna, 2004).

252 Rockpool pH and salinity fell to levels likely to produce carbonate undersaturation (Fig. 3; Kim

253 et al., 2014; Proum et al., 2018).

254

255 Shell length, shape, and erosion varied greatly between the acidified and reference sites,

256 whereas tissue and shell masses were similar (A4). Acidified water exposure does not always

257 cause shell mass reduction in gastropods (Marshall et al., 2008; Lardies et al., 2014; Chen et

258 al., 2015). Shell growth depends on both carbonate saturation of the surrounding water and

259 feeding opportunities (in turn affecting energetic status), whereas dissolution relates solely to

260 the external saturation state. We recorded shell-shortening and more globular-shaped shells in

261 acidified-site populations of *P. sulcatus* (Fig. 5). In these snails there was apical and upper-

262 spire erosion as well broadening of the shell aperture. Basal broadening likely relates to slower

263 growth in the acidified areas.

264 Gastropod shell surface erosion was a sensitive marker of acidification by recording shell loss

265 that was not readily detectable gravimetrically. This finding extends the known benefits of this

266 biomarker of seawater acidity from oceanic and estuarine gastropods (Marshall et al., 2008;

267 Bednaršek et al., 2012a, 2012b, 2014) to rocky shore animals and ecosystems. Our manually-

268 assessed eroded surface area for *N. chamaeleon* correlated with that computed digitally,

269 although the latter was more accurate as it accounted for small eroded areas between shell ribs.

270 Shell erosion ranking sharply distinguished acidified and reference sites. Median scores for *N.*

271 *chamaeleon* from references sites were half the value of those for acidified sites (Fig. 8), and

272 similar clear distinction was found for *P. sulcatus* (Fig. 9). Frequency distributions show that

273 that the highest erosion ranks only occur in the low pH sites (Figs 8 and 9). The few cases of

274 low erosion ranks at the acidified sites may represent within-shore movement, whereby snails

275 initially inhabiting higher pH water lower on the shore had recently moved into the more

276 acidified higher-shore habitats.

277 Whereas the number of ranks and the value ascribed to each rank are arbitrary, variation in

278 rank frequency across habitats is important. Despite using different approaches to rank shell

279 erosion, both species showed high frequencies of unique highest (or higher) ranks in acidifed

280 site populations (> 0.4), suggesting similarity in their acidification biomonitoring potential.

281   Our system can however be tailored to the scope and precision needs of an investigation. For
282   instance, it is possible to get three-dimensional information about erosion, by integrating
283   dissolution areas with shell thickness measurements (Figs 2 and 3). Although we focused on
284   measuring and ranking the areas of eroded shell surfaces, shell erosion could be estimated from
285   a spiral growth line superimposed on apically-viewed shell images (A6). Erosion could be
286   measured in terms of the ratio of the line length between the growing edge and the eroded shell
287   against the entire growth line (A6). Improvements could also involve integrating shell growth
288   rate and mineralogy of the study species with shell erosion measures.

289   **5. Appraisal of the biomonitoring tool**

290   Gastropod shell erosion as a biomonitoring tool has advantages over buoys fitted with loggers.
291   We were able to use benthic gastropods in intertidal habitats and because they are usually slow
292   moving or sedentary (occupying meter-sized areas), they can be used to monitor acidification
293   over a range of spatial scales, from metres to hundreds of kilometres. Sampling across a region
294   allows identification of areas with greater or lesser impacts of acidification. In addition to
295   recording chronic exposure of individuals, this approach to biomonitoring can compare
296   populations over time (see A7). Assessments of shell erosion are cost-effective and simple to
297   execute without requiring meters or instruments, such that this could gain the involvement and
298   benefits of citizen science (Dickinson et al., 2010; Gaston et al., 2018). Moreover, information
299   on acidification experienced by individual organisms using shell erosion ranking can be related
300   to other parameters (mass, age, growth and reproduction) of the same organism in the field.

301

302   There are important considerations when using shell erosion as a biomarker of seawater
303   acidification. Because time is a function of acidified seawater exposure, similar-aged
304   individuals (such as adults) should be used in biomonitoring exercises. Distinguishing shell
305   dissolution from weathering and bioerosion is not trivial (Schönberg et al., 2017). Shells
306   become worn through daily cycles of heating, cooling, wetting and drying which increase with
307   increasing vertical shore height (Underwood, 1979; Denny, 1988). Shell abrasion also
308   increases with more wave action and/or exposure to suspended sediments (Denny, 1988). It is
309   possible to tell the effects of bioerosion and erosion by acidified water apart, with the
310   characteristic pits and burrows of microborers often becoming conspicuous on shells.
311   Weathering, bioerosion and chemical erosion work together in acidified waters and are
312   accelerated if outer protective layers of the shell are lost. This problem can be surpassed by
313   establishing reference sites that show what shells are like in normal conditions as compared to

314 acidified conditions. In any event, gross shell erosion (as indicated by maximum SER values,
315 Figs 8 and 9), shell deformities and corroded shells in juveniles are independently clear signs
316 of acidified water exposure (Hall-Spencer et al., 2008; Marshall et al., 2008, 2016; Harvey et
317 al., 2018). Notably, gross shell erosion follows exposure to undersaturated carbonate
318 conditions irrespective of the processes driving these, thus this biomarker informs about a
319 change in environmental conditions and not the underlying mechanism.

320 Information on the ecology and biology of biomonitor species is crucial (Phillips and Rainbow,
321 1995). Species attributes such as shell size and thickness, mineralogy, growth rate, animal
322 behaviour and distribution are all important considerations. Biomonitoring potential is likely
323 to vary between gastropod species considering that mineralogy intrinsically influences natural
324 weathering. Local abundance and geographical distribution of a species add value to its use as
325 a biomonitor. Our study species are common rocky intertidal inhabitants and can potentially
326 be used to monitor acidificaiton across the vast Central Indo-Pacific ecoregion (Spalding et al.
327 2007; Palomares and Pauly, 2019). The methods we propose nonetheless provide a framework
328 for developing acidification biomonitoring using other gastropod species across a wide
329 spectrum of marine environments.

330 **6. Conclusions**

331 We show that gastropod shells can be used to assess the presence and effects of acidification
332 in nearshore and benthic coastal marine environments. This has advantages over conventional
333 monitoring in heterogeneous intertidal systems and allows the identification of critically-
334 exposed areas. In addition to indicating acidic discharges into coastal ecosystems, such
335 biomonitoring could help assess the extent of anthropogenic ocean acidification. Though some
336 refinement and standardization of protocols is required, gastropods show potential for
337 biomonitoring of acidification in marine ecosystems.

338 **7. Acknowledgments**

343 **8. Author contributions**

DJM conceived the original idea and JH-S further contextualized this; DJM and DTTW devised methods and approaches; DJM and NM collected, photographed and measured snails; LCDS developed the automated segmentation technique; SG provided input on the geology of the area as well as the supplementary figures. AAA undertook geometric morphometric analysis. All authors contributed to preparing and critically commenting on the manuscript.

9. Conflicts of Interest: The authors declare no conflicts of interest

10. References

Abdelhady, A.A., 2016. Phenotypic differentiation of the Red Sea gastropods in response to the environmental deterioration: geometric morphometric approach. J. Afr. Earth Sci. 115, 191–202.

Abdelhady, A.A., Abdelrahman, E., Elewa, A.M.T., Fan, J., Zhang, S., Xiao, J., 2018. Phenotypic plasticity of the gastropod *Melanoides tuberculata* in the Nile Delta: A pollution-induced stabilizing selection. Mar. Pollut. Bull. 133, 701–710. https://doi.org/10.1016/j.marpolbul.2018.06.026

Abdelhady, A.A., Fürsich, F.T., 2014. Macroinvertebrate palaeo-communities from the Jurassic succession of Gebel Maghara (Sinai, Egypt). J. African Earth Sci. 97, 173–193. https://doi.org/10.1016/j.jafrearsci.2014.04.019

Abdelhady, A.A., Fürsich, F.T., 2015. Sequence architecture of a Jurassic ramp succession from Gebel Maghara (North Sinai, Egypt): Implications for eustasy. J. Palaeogeogr. 4, 305–330. https://doi.org/10.1016/j.jop.2015.08.008

Azhar, A.S., Latiff, A.H.A., Lim, L.H., Gödeke, S.H., 2019. Groundwater investigation of a coastal aquifer in Brunei Darussalam using seismic refraction. Environ. Earth Sci. 78, 220. https://doi.org/10.1007/s12665-019-8203-6

Bednaršek, N., Feely, R.A., Reum, J.C.P., Peterson, B., Menkel, J., Alin, S.R., Hales, B., 2014. *Limacina helicina* shell dissolution as an indicator of declining habitat suitability owing to ocean acidification in the California Current Ecosystem. Proc. R. Soc. B Biol. Sci. 281, 20140123–20140123. https://doi.org/10.1098/rspb.2014.0123

376

377 Bednaršek, N., Tarling, G.A., Bakker, D.C.E., Fielding, S., Cohen, A., Kuzirian, A., McCorkle,

378 D., Lézé, B., Montagna, R., 2012b. Description and quantification of pteropod shell

379 dissolution: a sensitive bioindicator of ocean acidification. Glob. Chang. Biol. 18, 2378–2388.

380 https://doi.org/10.1111/j.1365-2486.2012.02668.x

381

382 Bednaršek, N., Tarling, G.A., Bakker, D.C.E., Fielding, S., Jones, E.M., Venables, H.J., Ward,

383 P., Kuzirian, A., Lézé, B., Feely, R.A., Murphy, E.J., 2012a. Extensive dissolution of live

384 pteropods in the Southern Ocean. Nat. Geosci. 5, 881–885. https://doi.org/10.1038/ngeo1635

385

386 Begliomini, F.N., Maciel, D.C., de Almeida, S.M., Abessa, D.M., Maranho, L.A., Pereira, C.S.,

387 Yogui, G.T., Zanardi-Lamardo, E., Castro, Í.B., 2017. Shell alterations in limpets as putative

388 biomarkers for multi-impacted coastal areas. Environ. Pollut. 226, 494–503.

389 https://doi.org/10.1016/j.envpol.2017.04.045

390

391 Bolhuis, H., Schluepmann, H., Kristalijn, J., Sulaiman, Z., Marshall, D.J., 2014. Molecular

392 analysis of bacterial diversity in mudflats along the salinity gradient of an acidified tropical

393 Bornean estuary (South East Asia). Aquat. Biosyst. 10, 1–13. https://doi.org/10.1186/2046-

394 9063-10-10

395

396 Cai, W.-J., 2011a. Estuarine and coastal ocean carbon paradox: CO_2 sinks or sites of terrestrial

397 carbon incineration? Ann. Rev. Mar. Sci. 3, 123–145. https://doi.org/10.1146/annurev-marine-

398 120709-142723

399

400 Cai, W.-J., Hu, X., Huang, W.-J., Murrell, M.C., Lehrter, J.C., Lohrenz, S.E., Chou, W.-C.,

401 Zhai, W., Hollibaugh, J.T., Wang, Y., Zhao, P., Guo, X., Gundersen, K., Dai, M., Gong, G.-

402 C., 2011b. Acidification of subsurface coastal waters enhanced by eutrophication. Nat. Geosci.

403 4, 766–770. https://doi.org/10.1038/ngeo1297

404

405 Chen, Y.J., Wu, J.Y., Chen, C.T.A., Liu, L.L., 2015. Effects of low-pH stress on shell traits of

406 the dove snail, *Anachis misera*, inhabiting shallow-vent environments off Kueishan Islet,

407 Taiwan. Biogeosci. 12, 2631–2639. https://doi.org/10.5194/bg-12-2631-2015

408

409 Connell, S.D., Doubleday, Z.A., Hamlyn, S.B., Foster, N.R., Harley, C.D.G., Helmuth, B.,

410 Kelaher, B.P., Nagelkerken, I., Sarà, G., Russell, B.D., 2017. How ocean acidification can

411 benefit calcifiers. Curr. Biol. 27, R95–R96. https://doi.org/10.1016/j.cub.2016.12.004

412

413 Denny, M., 1988. Biology and the mechanics of the wave swept environment. Princeton

414 University Press, New Jersey.

415

416 Dickinson, J.L, Zuckerberg, B., Bonter, D.N., 2010. Citizen science as an ecological research

417 tool: challenges   and   benefits.   Annu.   Rev.   Ecol.   Syst.   41,   49-172,

418 https://doi.org/10.1146/annurev-ecolsys-102209-144636

419

420 Doubleday, Z.A., Nagelkerken, I., Connell, S.D., 2017. Ocean life breaking rules by building

421 shells   in   acidic   extremes.   Curr.   Biol.   27,   R1104–R1106.

422 https://doi.org/10.1016/j.cub.2017.08.057

423

424 Duarte, C.M., Hendriks, I.E., Moore, T.S., Olsen, Y.S., Steckbauer, A., Ramajo, L., Carstensen,

425 J., Trotter, J.A., McCulloch, M., 2013. Is ocean acidification an open-ocean syndrome?

426 Understanding anthropogenic impacts on seawater pH. Estuaries and Coasts 36, 221–236.

427 https://doi.org/10.1007/s12237-013-9594-3

428

429 Duquette, A., McClintock, J.B., Amsler, C.D., Pérez-Huerta, A., Milazzo, M., Hall-Spencer,

430 J.M., 2017. Effects of ocean acidification on the shells of four Mediterranean gastropod species

431 near   a CO_2 seep.   Mar.   Pollut.   Bull.   124,   917–928.

432 https://doi.org/10.1016/j.marpolbul.2017.08.007

433

434 Garilli, V., Rodolfo-Metalpa, R., Scuderi, D., Brusca, L., Parrinello, D., Rastrick, S.P.S.,

435 Foggo, A., Twitchett, R.J., Hall-Spencer, J.M., Milazzo, M., 2015. Physiological advantages

436 of dwarfing in surviving extinctions in high-CO_2 oceans. Nat. Clim. Chang. 5, 678–682.

437 https://doi.org/10.1038/nclimate2616

438

439 Gaston, K.J., Soga, M., Duffy, J.P., Garrett, J.K., Gaston, S., Cox, D.T.C., 2018. Personalized

440 ecology. TREE, 33, 916–925.

441

442 Gibbs, P.E., Bryan, G.W., Pascoe, P.L., Burt, G.R., 1987. The use of the dog-whelk, *Nucella*
443 *lapillus*, as an indicator of tributyltin (TBT) contamination. J. Mar. Biol. Assoc. United
444 Kingdom 67, 507–523. https://doi.org/10.1017/S0025315400027260

446 Grealish, G.J., Fitzpatrick, R.W., 2013. Acid sulphate soil characterization in Negara Brunei
447 Darussalam: a case study to inform management decisions. Soil Use Manag. 29, 432–444.
448 https://doi.org/10.1111/sum.12051

450 Hall-Spencer, J.M., Rodolfo-Metalpa, R., Martin, S., Ransome, E., Fine, M., Turner, S.M.,
451 Rowley, S.J., Tedesco, D., Buia, M-C. 2008. Volcanic carbon dioxide vents show ecosystem
452 effects of ocean acidification. doi:10.1038/nature07051

454 Hammer, Ø., Harper, D.A.T., Ryan, P.D., 2001. PAST: paleontological statistics software
455 package for education and data analysis. Palaeontol. Electronica 4, 1–9.

457 Harvey, B.P., Agostini, S., Wada, S., Inaba, K., Hall-Spencer, J.M., 2018. Dissolution: the
458 Achilles' heel of the Triton shell in an acidifying ocean. Front. Mar. Sci. 5, 1–11.
459 https://doi.org/10.3389/fmars.2018.00371

461 Harvey, B.P., McKeown, N.J., Rastrick, S.P.S., Bertolini, C., Foggo, A., Graham, H., Hall-
462 Spencer, J.M., Milazzo, M., Shaw, P.W., Small, D.P., Moore, P.J., 2016. Individual and
463 population-level responses to ocean acidification. Sci. Rep. 6, 20194.
464 https://doi.org/10.1038/srep20194

466 Hossain, M.B., Marshall, D.J., 2014. Benthic infaunal community structuring in an acidified
467 tropical estuarine system. Aquat. Biosyst. 10, 11. https://doi.org/10.1186/2046-9063-10-11

469 Hossain, M.B., Marshall, D.J., Venkatramanan, S., 2014. Sediment granulometry and organic
470 matter content in the intertidal zone of the Sungai Brunei estuarine system, northwest coast of
471 Borneo. Carpathian J. Earth Environ. Sci. 9, 231–239.

473 Lardies, M.A., Arias, M.B., Poupin, M.J., Manríquez, P.H., Torres, R., Vargas, C.A., Navarro,
474 J.M., Lagos, N.A., 2014. Differential response to ocean acidification in physiological traits of

Concholepas *concholepas* populations. J. Sea Res. 90, 127–134. https://doi.org/10.1016/j.seares.2014.03.010

Majewska, R., Adam, A., Mohammad-Noor, N., Convey, P., De Stefano, M., Marshall, D.J., 2017. Spatio-temporal variation in phytoplankton communities along a salinity and pH gradient in a tropical estuary (Brunei, Borneo, South East Asia). Trop. Ecol. 58, 251–269.

Marshall, D.J., Aminuddin, A., Ahmad, S., 2018. Gastropod diversity at Pulau Punyit and the nearby shoreline - a reflection of Brunei's vulnerable rocky intertidal communities. Sci. Bruneiana 17, 34–40.

Marshall, D.J., Proum, S., Hossain, M.B., Adam, A., Hoon Lim, L., Santos, J.H., 2016. Ecological responses to fluctuating and extreme marine acidification: lessons from a tropical estuary (the Brunei Estuarine System). Sci. Bruneiana Special Is, 1–12.

Marshall, D.J., Santos, J.H., Leung, K.M.Y., Chak, W.H., 2008. Correlations between gastropod shell dissolution and water chemical properties in a tropical estuary. Mar. Environ. Res. 66, 422–429. https://doi.org/10.1016/j.marenvres.2008.07.003

Márquez, F., Nieto Vilela, R.A., Lozada, M., Bigatti, G., 2015. Morphological and behavioral differences in the gastropod *Trophon geversianus* associated to distinct environmental conditions, as revealed by a multidisciplinary approach. J. Sea Res. 95, 239–247. https://doi.org/10.1016/j.seares.2014.05.002

Morley, C.K., Back, S., Van Rensbergen, P., Crevello, P., Lambiase, J.J., 2003. Characteristics of repeated, detached, Miocene–Pliocene tectonic inversion events, in a large delta province on an active margin, Brunei Darussalam, Borneo. J. Struct. Geol. 25, 1147–1169. https://doi.org/10.1016/S0191-8141(02)00130-x

Nuñez, J.D., Laitano, M. V., Cledón, M., 2012. An intertidal limpet species as a bioindicator: Pollution effects reflected by shell characteristics. Ecol. Indic. 14, 178–183. https://doi.org/10.1016/j.ecolind.2011.07.015

508   Palomares, M.L.D. and D. Pauly. Editors. 2019. SeaLifeBase. World Wide Web electronic
509   publication. www.sealifebase.org, version (04/2019)

511   Phillips, D.J.H., Rainbow, P.S., 1993. Biomonitoring of trace aquatic contaminants. Springer
512   Netherlands, Dordrecht, pp. 133–178. https://doi.org/10.1007/978-94-011-2122-4_6

514   Powell, B., Martens, M., 2005. A review of acid sulfate soil impacts, actions and policies that
515   impact on water quality in Great Barrier Reef catchments, including a case study on
516   remediation at East Trinity. Mar. Pollut. Bull. 51, 149–164.
517   https://doi.org/10.1016/j.marpolbul.2004.10.047

519   Proum, S., Harley, C.D., Steele, M., Marshall, D.J., 2017. Aerobic and behavioral flexibility
520   allow estuarine gastropods to flourish in rapidly changing and extreme pH conditions. Mar.
521   Biol. 164, 97. https://doi.org/10.1007/s00227-017-3124-y

523   Proum, S., Santos, J.H., Lim, L.H., Marshall, D.J., 2016. Metal accumulation in the tissues and
524   shells of *Indothais gradata* snails inhabiting soft and hard substrata in an acidified tropical
525   estuary (Brunei, South East Asia). Reg. Stud. Mar. Sci. 8, 487–497.
526   https://doi.org/10.1016/j.rsma.2016.03.010

528   Proum, S., Santos, J.H., Lim, L.H., Marshall, D.J., 2018. Tidal and seasonal variation in
529   carbonate chemistry, pH and salinity for a mineral-acidified tropical estuarine system. Reg.
530   Stud. Mar. Sci. 17, 17–27. https://doi.org/10.1016/j.rsma.2017.11.004

532   Rohlf, F.J., 1996. Morphometric spaces, shape components and the effects of linear
533   transformations, in: Marcus, L.F., Corti, M., Loy, A., Naylor, G.J.P., Slice, D.E. (Eds.),
534   Advances in Morphometrics. Springer US, Boston, MA, pp. 117–129.
535   https://doi.org/10.1007/978-1-4757-9083-2_11

537   Rohlf, F.J., Slice, D., 1990. Extensions of the Procrustes method for the optimal
538   superimposition of landmarks. Syst. Biol. 39, 40–59. https://doi.org/10.2307/2992207

540 Schönberg, C.H.L., Fang, J.K.H., Carreiro-Silva, M., Tribollet, A., Wisshak, M., 2017.

541 Bioerosion: the other ocean acidification problem. ICES J. Mar. Sci. 74, 895–925.

542 https://doi.org/10.1093/icesjms/fsw254

543

544 Spalding, M.D., Fox, H.E., Allen, G.R., Davidson, N., Ferdaña, Z.A., Finlayson, M., Halpern,

545 B.S., Jorge, M.A., Lombana, A., Lourie, S.A., Martin, K.D., Mcmanus, E., Molnar, J., Recchia,

546 C.A., Robertson, J., 2007. Marine ecoregions of the world: A bioregionalization of coastal and

547 shelf areas. Bioscience, 57, 573-583.

548

549 Underwood, A.J., 1979. The ecology of intertidal gastropods. Adv. Mar. Biol. 16, 111–210.

550 https://doi.org/10.1016/S0065-2881(08)60293-x

551

552 Urish, D.W., McKenna, T.E., 2004. Tidal effects on ground water discharge through a sandy

553 marine beach. Ground Water 42, 971–982. https://doi.org/10.1111/j.1745-

554 6584.2004.tb02636.x

555

556 Waska, H., Greskowiak, J., Ahrens, J., Beck, M., Ahmerkamp, S., Böning, P., Brumsack,

557 H.J., Degenhardt, J., Ehlert, C., Engelen, B., Grünenbaum, N., Holtappels ,M., Pahnke, K.,

558 Marchant, H.K., Massmann, G., Meier, D., Schnetger B., Schwalfenberg, K., Simon,

559 H., Vandieken, V., Zielinski, O., Dittmar, T. 2019. Spatial and temporal patterns of pore water

560 chemistry in the inter-tidal zone of a high energy beach. Front. Marine. Sci.

561 https://doi.org/10.3389/fmars.2019.00154

562

563 Zelditch, M.L, Swiderski, D.L., Sheets, H.D., 2012. Geometric morphometrics for biologists:

564 A primer. Elsevier Academic Press, London.

565

566 Zhai, W.-D., Zang, K.-P., Huo, C., Zheng, N., Xu, X.-M., 2015. Occurrence of aragonite

567 corrosive water in the North Yellow Sea, near the Yalu River estuary, during a summer flood.

568 Estuar. Coast. Shelf Sci. 166, 199–208. https://doi.org/10.1016/j.ecss.2015.02.010

569

570 Zhou, Q., Zhang, J., Fu, J., Shi, J., Jiang, G., 2008. Biomonitoring: an appealing tool for

571 assessment of metal pollution in the aquatic ecosystem. Anal. Chim. Acta 606, 135–150.

572 https://doi.org/10.1016/j.aca.2007.11.018

573

574

575

576

577

578

579

580

581

Figure captions

Figure 1. Physical map showing sampling sites and waterways in Brunei Darussalam (Borneo, South East Asia). JPMC (Jerudong Park Medical Centre), 4°56'55'' N, 114°49'42''E; PJER (Pantai Jerudong), 4°57'30'' N, 114°50'22''E; PUN (Punyit), 4° 58' 30.3996" N, 114° 50' 56.7996"E; E1 (Empire), 4°58'08'' N, 114°51'18''E; E2 (Empire), 4°58'05'' N, 114°51'20''E; E3 (Empire), 4°58'05'' N, 114°51'19''E; TP (Pantai Tungku), 4°58'13'' N, 114°52'00''E; UB (Universiti Brunei Darussalam), 4°59'07'' N, 114°53'58''E.

Figure 2. Shell erosion ranking in *Nerita chamaeleon* (apical view). A quadrant and seven sectors based on the shell growth pattern were established from a line drawn between the columella notch (b) and the apex (circled a). The apex is the oldest shell with the growing edge (labelled c) in sector 7. Two depths (types) of erosion were scored, Type I is deep erosion to the fine textured, grey/white layer and Type II is superficial erosion of the pigmented, ridged layer under the periostracum. A score was based on the highest sector showing > 50% eroded shell. Shell A shows no erosion with the periostracum intact to the apex, shell B shows a ruffled periostracum covering > 50% of sector 6 (scores 5 for Type II) and shell C shows complete Type I erosion in sector 5 and complete Type II erosion in sector 7.

Figure 3. Shell erosion ranking in *Planaxis sulcatus* (abapertural view). R1 (not shown), shell whorls 1 and 2 (W1, W2) intact with fine ridges; R2, complete or incomplete ridges on W3; R3, W3 completely worn but W4 mostly ridged; R4, W4 mostly to completely worn but body whorl (WB) completely ridged; R5, WB eroded towards the right edge.

Figure 4. Upper and middle. pH and salinity at acidified sites E1, E2 and E3 and reference sites, JMPC, PJER and PUN (n = 103). TP and UB were similar to other reference sites (pH was 8.44 – 8.29 and salinity was 33.1 – 31 psu; n = 21). Bottom. Relationship between pH and salinity at the acidified sites, with boxes showing conditions likely to cause calcite (Ca) or aragonite (Ar) undersaturation (see Proum et al., 2018).

Figure 5. 2D-DCA plot (axes 1 *vs.* axis 2) for *P. sulcatus* shells from an acidified site (E2, blue squares) and reference sites (UB, red crosses and TP, green crosses). TPS deformation grids represent individuals located at both extremes of the x and y axes. The population from the acidified site (E2, blue squares) overlaps weakly with reference populations. Correlations show that DC1 is especially influenced by aperture shape and DC2 by shell height. ANOSIM results were UB/E2, p = 0.01; UB/TP, p = 0.0177; E2/TP, p = 0.0001.

Figure 6. Eroded and total abapertural surface areas of *N. chamaeleon* shells from PUN (reference, blue, n = 25) and E1 (acidified, red, n = 15), determined manually (A, B, C; mean $\pm$ 1 s.e.m). (D) Number of individuals with eroded (> 10%) and non-eroded shells.

Figure 7. Examples showing red-blue-white colour partitioning of shell surfaces, used in the automated determination of percentage shell erosion (upper). Pixel numbers and percentage erosion calculations are shown. A least squares linear regression relating manually and digitally determined percentage erosion (lower).

Figure 8. *Nerita chamaeleon* shell erosion ranks (SER). (A) Box-Whisker plots and outliers of SERs for three acidified (E1, E2, E2) and three reference (JPMC, PJER, PUN) sites using combined Type I and II ranks (0-14). Different letters above plots indicate significant differences between sites (see Table 1). (B) Snail frequencies at each site for Type I rank (0-6).

Figure 9. *Planaxis sulcatus* shell erosion ranks (SER). (A) Box-Whisker plots and outliers of SERs for three acidified (E1, E2, E2) and three reference (JPMC, PJER, PUN) sites for apertural and abapertural surface ranks combined (2-10). Different letters above plots indicate significant differences between sites (see Table 1). (B) Snail frequencies at each site (ranks 2-5).